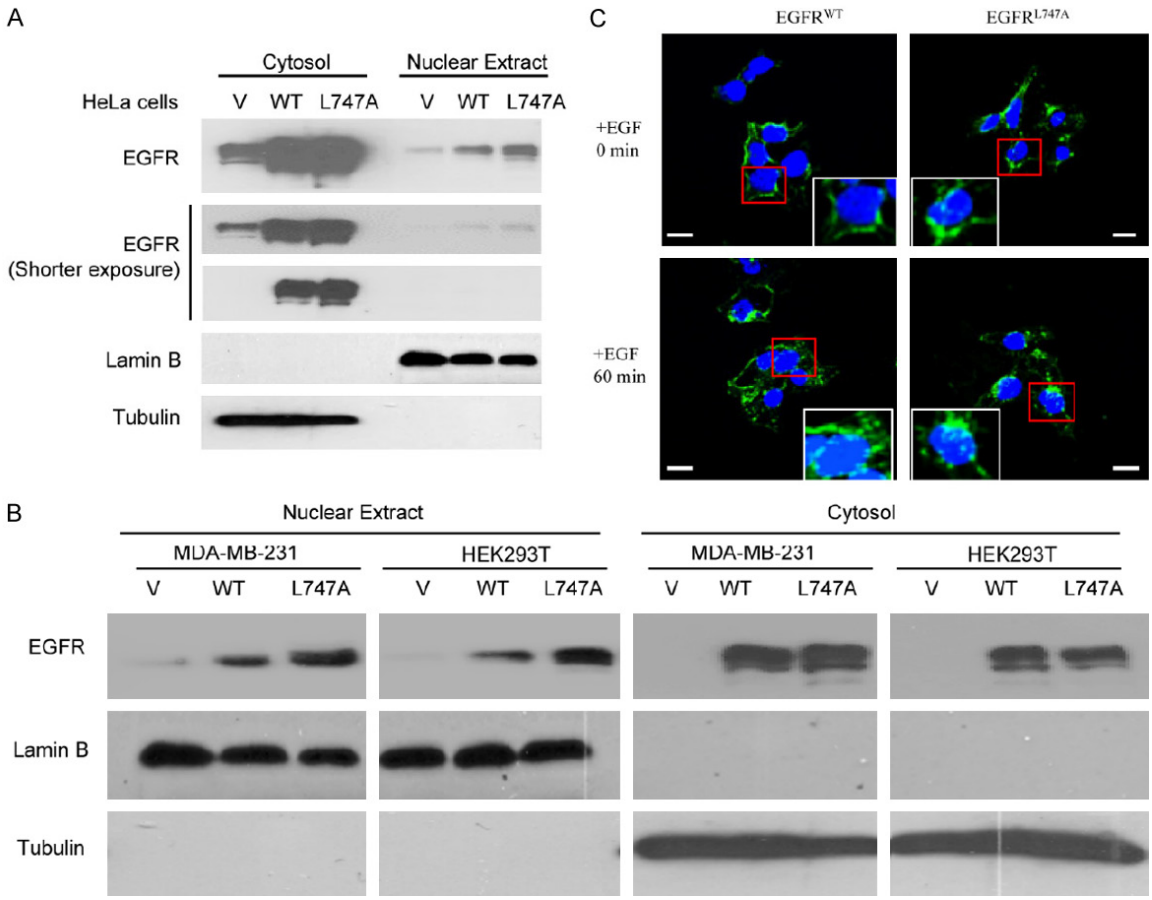

Figure S1. Mutation of EGFR at L747 increases its nuclear accumulation in human cancer cells. (A and B) Myc-tagged EGFR mutant-expressing plasmids were transient transfected into HeLa (A), MDA-MB-231 (B), and HEK293T (B) cells. The nuclear extract and cytosol were immunoblotted with the indicated antibodies. (C) HEK293T cells expressing GFP-fusion protein of EGFR WT and NES mutant (EGFR L747A) were starved overnight, and then stimulated with or without EGF (50 ng/ml) for 60 min. The cells were fixed and observed under confocal microscopy and representative images of nuclear localization were shown in insets. WT, wild-type. Bar, 10 μm.

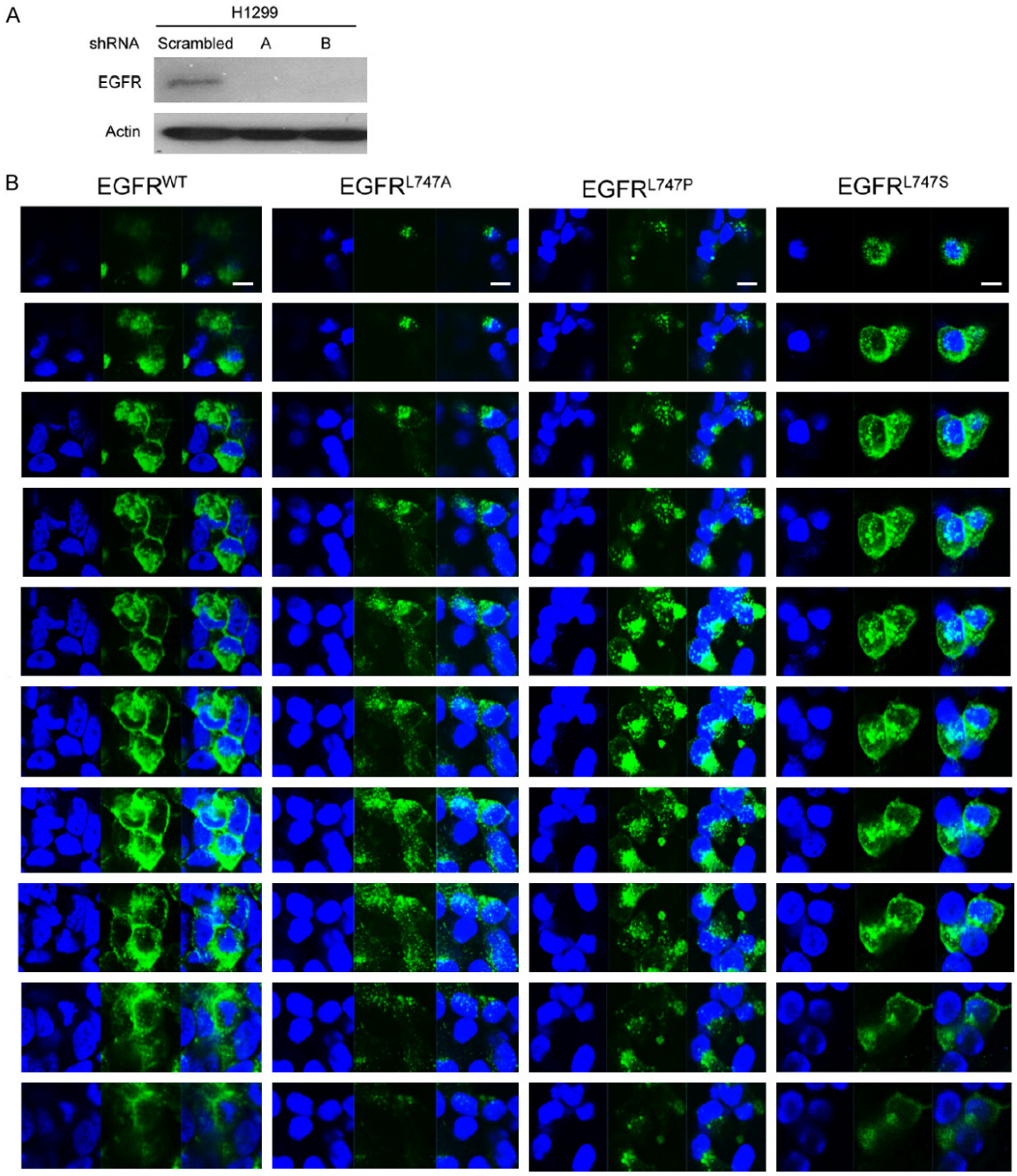

Figure S2. Confocal Z-stack scanning shows EGFR localization of H1299 cells expressing EGFR WT and L747 mutants in the nuclei. A. Knock-down of EGFR in H1299 cells with scrambled and shRNA EGFR-A and -B. B. H1299 cells expressing GFP-fused EGFR wild-type and L747 mutants were serum starved for 12 hours and stimulated with 60 ng/ml EGF for 30 min. The cells were fixed and permeabilized. The cell nuclei were visualized with DAPI. Confocal Z-stack scanning of the slides was performed using a LSM710 fluorescence confoca confocal microscope. Serial confocal images 1 μm apart along the Z axis were obtained. Bar, 10 μm.

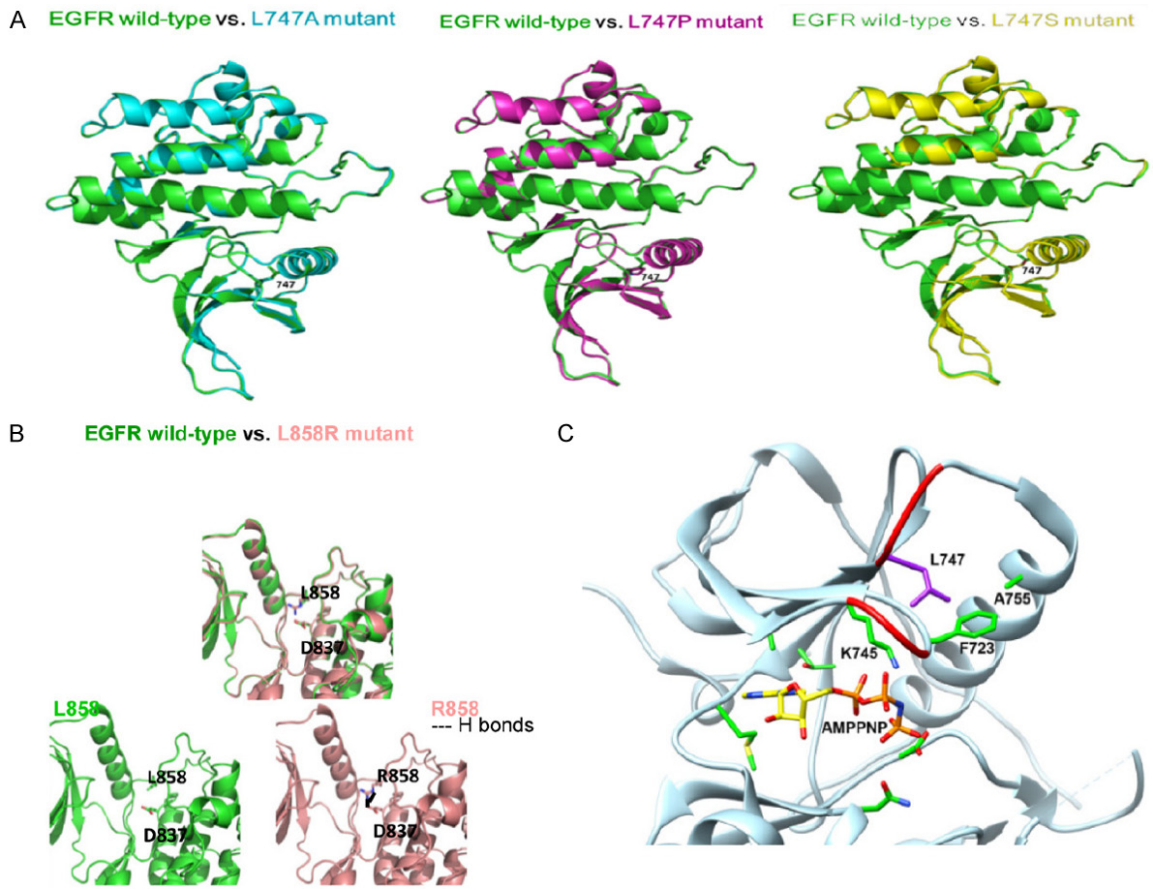

Figure S3. NES mutation of EGFR does not significantly affect 3D conformation of the kinase domain and ATP inhibitor binding site. A. The 3D model of the kinase domain of human EGFR L747 mutants were constructed using 1M17 as the template for homology modeling using the program (PS)2. The figures were produced by PyMOL. B. The inhibitor binding site of human EGFR L858R mutant kinase domain (PDB code 2ITV). C. The residue of L747 is colored purple; the key residues interacting with L747 or AMPPNP are colored green. The loop where L747 locates and P loop are shown in red ribbons. The AMPPNP molecule is displayed as the stick model with yellow C atoms. The figure was produced by using matchmaker tool of UCSF Chimera.

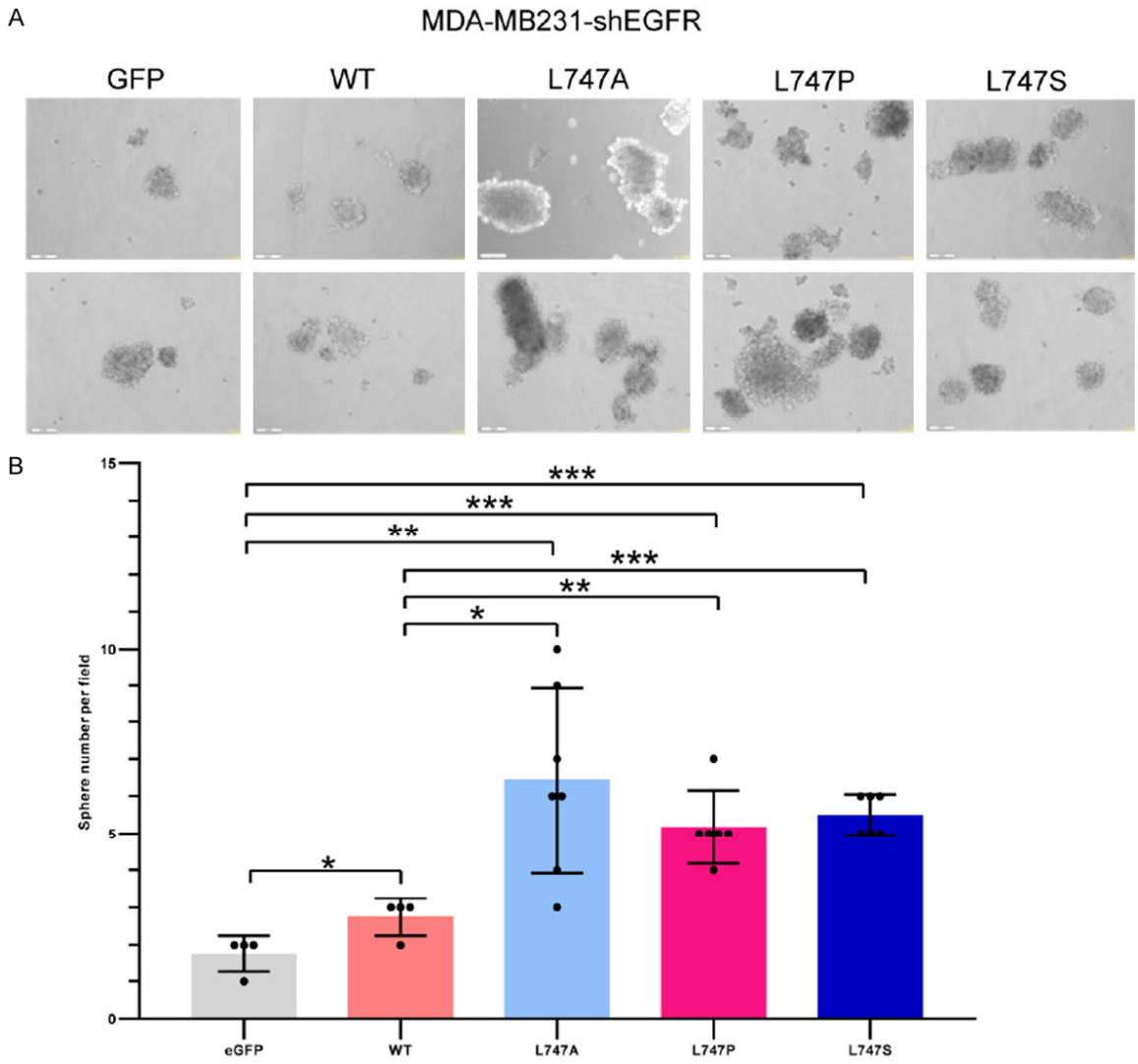

Figure S4. EGFR NES mutants significantly increase tumorsphere numbers in MDA-MB-231 cells. (A) MDA-MB-231 cells stably re-expressing EGFR WT and L747 mutants were performed in tumorsphere formation assay. Bar, 100 μm. (B) Bar graphs of tumorsphere numbers in (A) are presented as the mean value ± SE. *$p < 0.05$, **$p < 0.01$, ***$p < 0.001$.

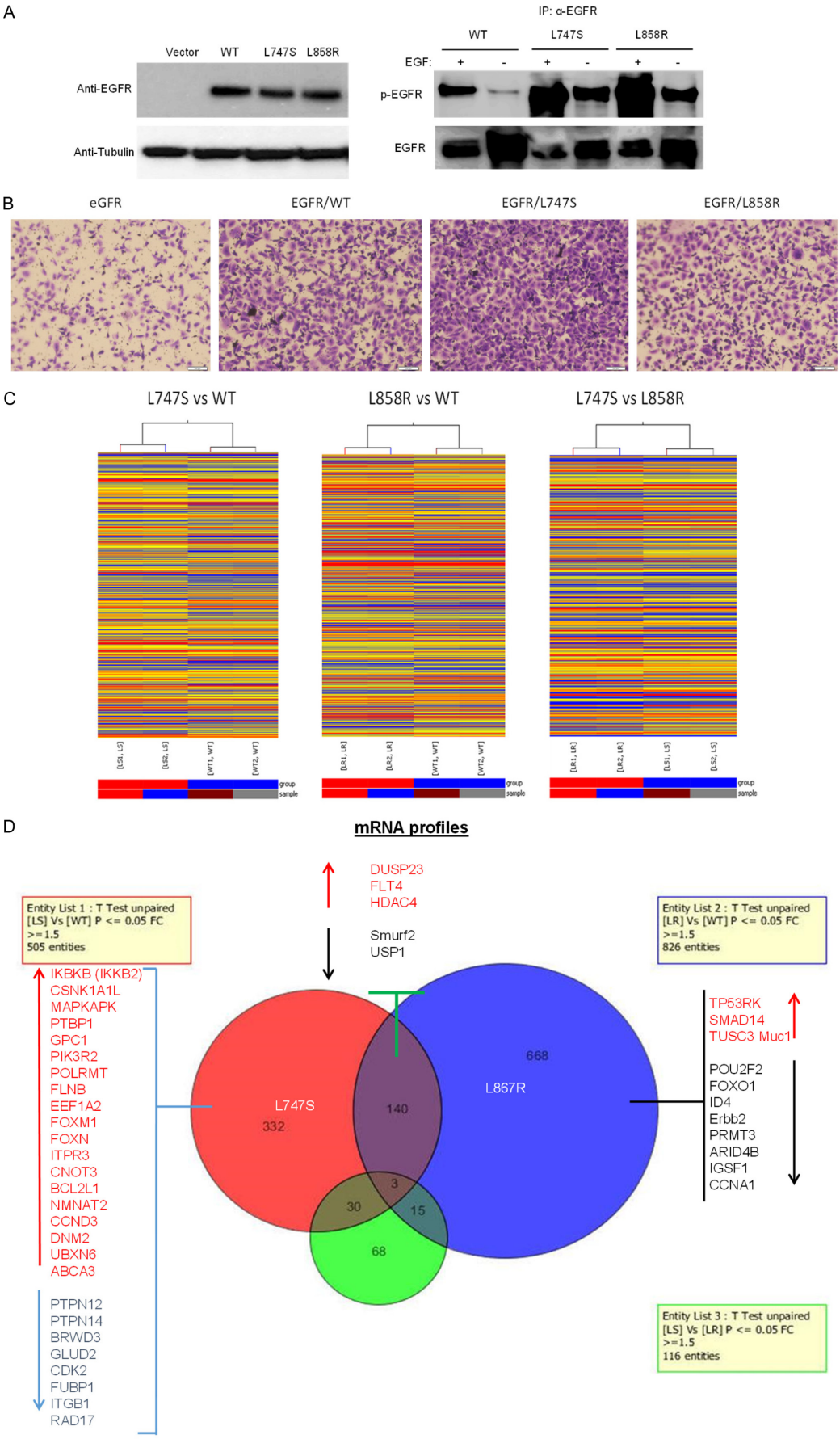
A
Vector
WT
L747S
L858R
Anti-EGFR
Anti-Tubulin
IP: α-EGFR
WT
L747S
L858R
EGF:
+
-
+
-
+
-
p-EGFR
EGFR
B
eGFR
EGFR/WT
EGFR/L747S
EGFR/L858R
C
L747S vs WT
L858R vs WT
L747S vs L858R
group
sample
D
mRNA profiles
Entity List 1 : T Test unpaired
[LS] Vs [WT] P <= 0.05 FC
>=1.5
505 entities
IKBKB (IKKB2)
CSNK1A1L
MAPKAPK
PTBP1
GPC1
PIK3R2
POLRMT
FLNB
EEF1A2
FOXM1
FOXN
ITPR3
CNOT3
BCL2L1
NMNAT2
CCND3
DNM2
UBXN6
ABCA3
PTPN12
PTPN14
BRWD3
GLUD2
CDK2
FUBP1
ITGB1
RAD17
DUSP23
FLT4
HDAC4
Smurf2
USP1
L747S
332
140
668
L867R
3
30
15
68
Entity List 2 : T Test unpaired
[LR] Vs [WT] P <= 0.05 FC
>=1.5
826 entities
TP53RK
SMAD14
TUSC3 Muc1
POU2F2
FOXO1
ID4
Erbb2
PRMT3
ARID4B
IGSF1
CCNA1
Entity List 3 : T Test unpaired
[LS] Vs [LR] P <= 0.05 FC
>=1.5
116 entities

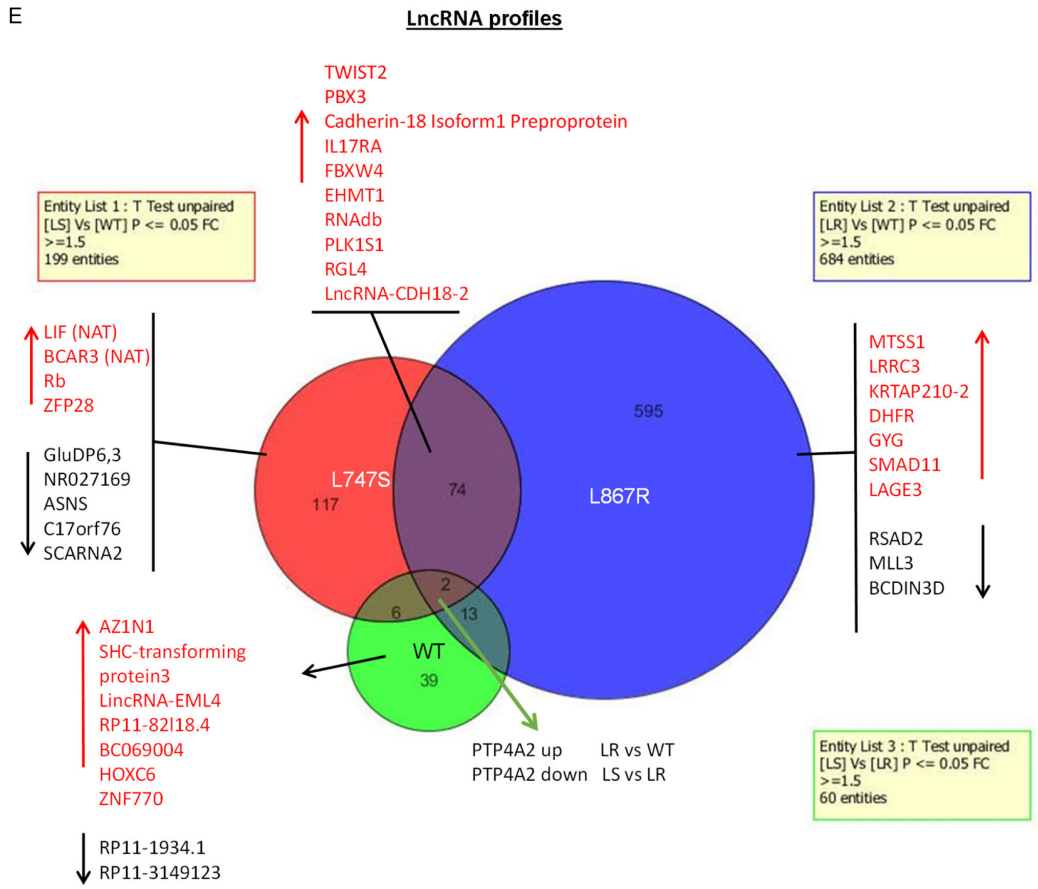

Figure S5. Transcriptome profiles of H1299 cells expressing EGFR^{WT}, EGFR^{L747S}, and EGFR^{L858R}. (A) Phosphorylated and total EGFR protein levels of the reconstituted expression of the WT and L747S and L858R mutants of EGFR were determined using immunoblotting analyses with indicated antibodies. (B) Invasive potential of the cell lines were determined using Boyden chamber assay. Bar, 200 μm. (C-E) Two sets of RNA samples from each stable cell line were used for statistical analysis. Total RNAs isolated from two sets of these stable cell lines were used for Microarray analyses. Heat maps of gene expression profiles (C), protein coding gene profiles (D), and long non-coding RNA (LncRNA) profiles (E) in the cell lines expressing EGFR^{WT}, EGFR^{L747S} and EGFR^{L858R}.

Table S2. Limiting-dilution transplantation assay of cancer cells expressing EGFR NES mutant and its nuclear translocation-deficient mutant

Cell line	Cell dilution	Mouse number	Tumor formation rate (%)
WT	1×10^5	6	3/6 (50)
	5×10^4	6	0/6 (0)
WT/AA	1×10^5	6	1/6 (16.7)
	5×10^4	6	0/6 (0)
L747P	1×10^5	6	5/6 (83.3)
	5×10^4	6	4/6 (66.7)
L747P/AA	1×10^5	6	2/6 (33.3)
	5×10^4	6	2/6 (33.3)
L747S	1×10^5	4	4/4 (100)
	5×10^4	6	5/6 (83.3)
L747S/AA	1×10^5	6	2/6 (33.3)
	5×10^4	6	2/6 (33.3)

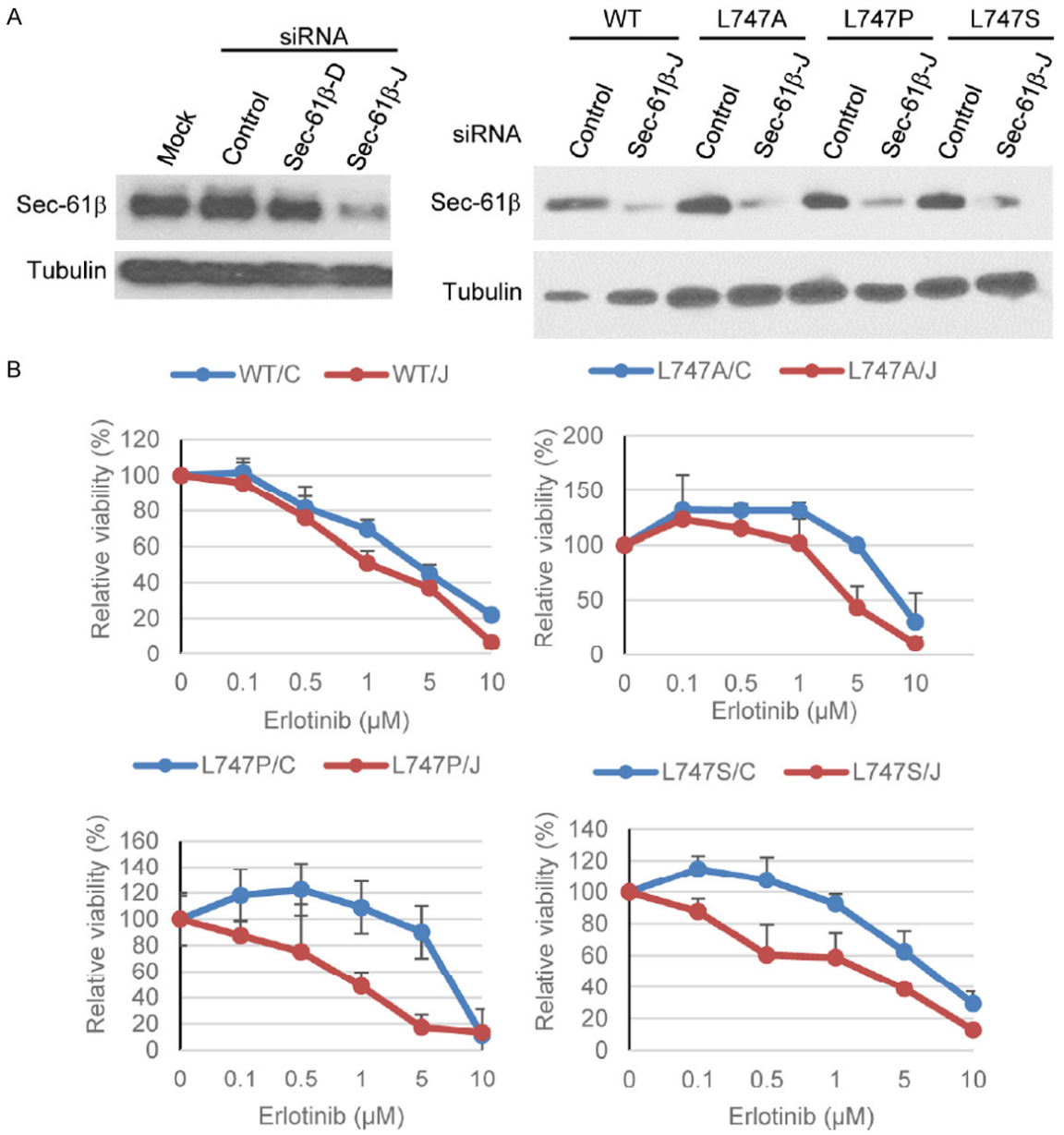

Figure S6. Blockade of nuclear translocation of EGFR sensitizes cancer cells to TKI. A. H1299 cells reconstituted expression of the indicated plasmids were transfected with siRNA-D and J against Sec61β and control siRNA (Themo Scientific Dhamacon), respectively. The cell lysates were immunoblotted with anti-Sec61β and anti-Tubulin. B. Viability assay of the H1299 cells reconstituted expression of EGFR WT and L747 mutants were incubated with erlotinib at different concentration for 72 h after knocking down Sec61β.

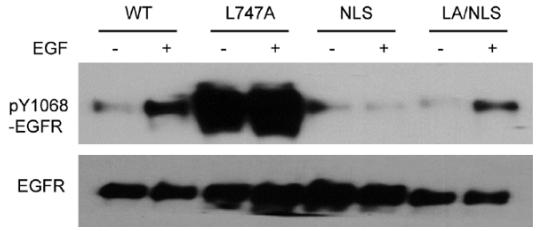

Figure S7. Deletion of the EGFR NLS motif abolishes EGFR kinase activity. Cells expressing the indicated plasmids, with or without EGF treatment, were immunoblotted with the indicated antibodies.

Table S3. Germline expression of EGFR NES mutant displays defect in breeding

F_0: L749P or L749S founders (transmitted to F_1)		
• $F_1^{+/-} \times F_1^{+/-}$	No pups (cannot get homozygotes)	
• $F_0 \times$ WT	F_1 offspring#	Predicted heterozygote#
	Total: 263	65.7 (25% probability)
$F_1^{+/-}$ (Heterozygotes) pup		15 (5.7%)
$X^2 = 39.1$	$p > 19.58 = 0.0001$	

Pathological phenotype: defect in breeding, hematopoietic tumor (B cell).

Table S4. Germline expression of membrane-bound EGFR mutant does not affect breeding

F_0: LL1012-1013	founders	
$F_0^{+/-} \times$ WT	F1 offsprings	21
	Heterozygote	4
	WT	17
$F_1^{+/-} \times F_1^{+/-}$	F2 offsprings	24
	Heterozygote	11
	Homozygote	9
	WT	4
	$p > 0.05$, NS	

Pathological phenotype: normal in breeding, no tumor.

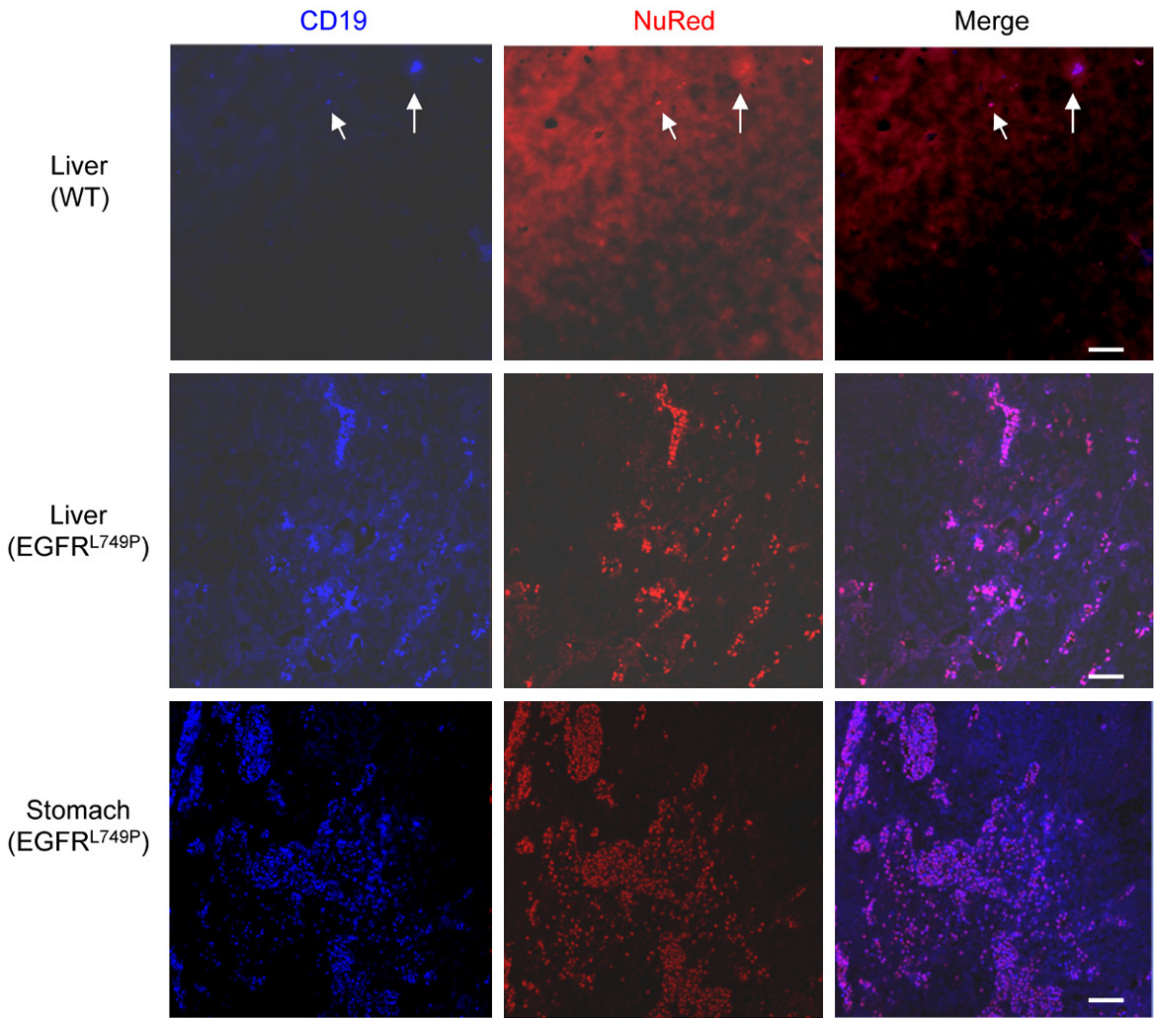

Figure S8. Germline expression of EGFR L749 mutant develops hematopoietic B cell lymphoma. Confocal images of B cell lineage marker staining of normal and tumor tissues. Normal and tumor tissues were fixed with paraformaldehyde and permeabilized with 4% NP-40, followed by 2.5% BSA blocking, and stained with Brilliant Violet 510™ anti-mouse CD19 and NucRedDead 647. Representative images were obtained using a LSM710 fluorescence confocal microscope. Bar, 50 μm.

Table S5. Somatic mutations of EGFR NES found in human B lymphocyte originated tumor (COSMIC database)

Sample ID	AA mutation	CDS mutation	Primary Tissue	Histology	Histology subtype	(Zygosity)
1998470	T751I	C2252C > T	Hematopoietic and lymphoid	Lymphoid neoplasm	Plasma cell myeloma	(Heterozygous)
1092628	T751I	C2252C > T	Hematopoietic and lymphoid	Lymphoid neoplasm	Plasma cell myeloma	(Heterozygous)
1998476	P753S	C2357C > T	Hematopoietic and lymphoid	Lymphoid neoplasm	Hairy cell leukemia	(Homozygous)
2426650	A750P	C?	Hematopoietic and lymphoid	Lymphoid neoplasm	Plasma cell myeloma	(Heterozygous)